Brazilian Journal of Physics (2021) 51:919–926
https://doi.org/10.1007/s13538-021-00865-z

SBF SOCIEDADE BRASILEIRA DE FÍSICA

ATOMIC PHYSICS

Overlapping Adding-Doubling Spikes Cascades in a Semiconductor Laser Proxy

Jason A. C. Gallas[1,2]

Received: 21 December 2020 / Accepted: 28 January 2021 / Published online: 25 April 2021

Abstract
A study of the distribution of spikes in periodic oscillations is reported for an optically injected laser diode proxy, as a function of the injected field strength and detuning. A novel and unexpected feature reported here is an abundance of overlapping adding-doubling complexification cascades. Two-parameter spikes complexification cascades of the laser proxy are found to mimic phenomena also found in a state-of-the-art semiconductor laser model. Such cascades should not be difficult to observe experimentally, either in lasers or in other complex oscillators.

Keywords Adding-doubling complexification · Complex oscillations · Semiconductor lasers · Stability diagrams

1 Introduction

The investigation of several natural phenomena is based on the observation of the temporal behavior of a dynamical variable of interest. After cataloguing the possible behaviors, the next important task is to catalogue what happens when control parameters are varied, namely, to delimit the size and the boundaries of the stability phases corresponding to the individual behaviors observed. A key feature of time-signals is their waveforms, which may be periodic or not. In general, nonisomorphic waveforms differ by the number p of spikes, i.e., local maxima, that they contain.

During a recent investigation [1] of a cancer growth model it was observed that, when two control parameters, say κ and ε, vary simultaneously, the transition boundaries between dynamical phases characterized by periodic time-signals having p spikes per period evolve in a startling regular way as depicted schematically in Fig. 1: When κ varies horizontally, a stability phase with, say, p spikes per period, transits sharply along a smooth path into a phase with $p+1$ spikes. In contrast, vertical variations of ε eventually lead to three distinct smooth transitions which occur at a first phase trifurcation level t_1: the emergence of a parabolic-shaped phase characterized by $2p+1$ spikes, the sum of the p and $p+1$ spikes of its precursor phases. This parabolic-shaped phase is flanked by two nonparabolic phases characterized by $2p$ and $2(p+1)$ spikes per period, as indicated in Fig. 1. By further varying ε one eventually reaches a second level t_2 when new phase trifurcations occur at both extremities of the parabolic arc, and so on.

In Fig. 1, all blue parabolic phases are invariably characterized by oscillations with an odd number of spikes, while the adjacent white non-parabolic phases contain an even number of spikes. Parabolic phases arise through spike additions, while nonparabolic phases arise from spike doublings. So far, the characteristic signature found for this regular adding-doubling complexification cascade is that the parabolic arcs do not overlap. For instance, in addition to the aforementioned cancer model [1], nonoverlapping adding-doubling cascades were observed subsequently in several rather distinct contexts, more recently in Refs. [2–6]. But, are overlapping adding-doubling cascades possible? What sort of dynamics should be expected when adding-doubling cascades overlap?

The aim of the present paper is to report a myriad of overlapping adding-doubling complexification cascades of spikes discovered in the control parameter space of a laser diode proxy for which Lyapunov stability diagrams were reported by Li et al. [7]. We find overlapping cascades to exist over broad parameter ranges. Since the proxy model considered here essentially coincides with a state-of-the-art

✉ Jason A. C. Gallas
jason.gallas@gmail.com

1 Instituto de Altos Estudos da Paraíba, Rua Silvino Lopes 419-2502, 58039-190 João Pessoa, Brazil

2 Complexity Sciences Center, 9225 Collins Avenue Suite 1208, Surfside, FL 33154, USA

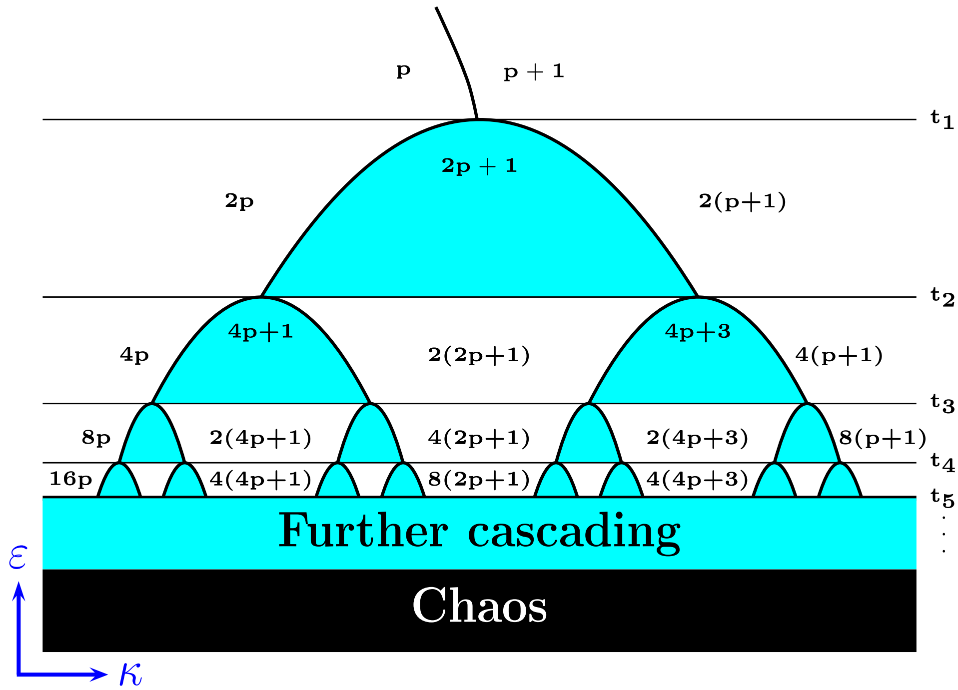

Fig. 1 Schematic unfolding of a nonoverlapping spikes adding-doubling complexification cascade, observed when two control parameters κ and ε vary simultaneously. Following a first phase trifurcation at t_1, one finds certain parabolic-shaped phases resulting from periodic oscillations with an odd number of spikes per period, while their adjacent phases have even number of spikes. The vertex of each parabola is a startling exceptional boundary point where five distinct oscillation phases meet. The further cascading is apparently finite and not especially long. Adapted from Ref. [1]

model of a semiconductor laser with optical injection, we expect overlapping adding-doubling cascades of spikes to be within reach of experimental observation with existing technology.

2 Model Equations

The state-of-the-art rate equation model of a single-mode diode laser with monochromatic optical injection and slowly varying complex electric field $E = x + iy$, and population inversion n is [8–11]

$$\dot{x} = \kappa + \omega y + \frac{1}{2}(x - \alpha y)n, \tag{1}$$

$$\dot{y} = -\omega x + \frac{1}{2}(\alpha x + y)n, \tag{2}$$

$$\dot{n} = -2\gamma n + (1 + 2Bn)\left(1 - x^2 - y^2\right), \tag{3}$$

where the κ is the injected field strength, and ω is the detuning of the injected field from the solitary laser frequency. The parameter α is the linewidth enhancement factor [12], while γ and B are material parameters: γ is the rescaled damping rate of the so-called relaxation oscillations, and B is the rescaled cavity lifetime of photons in the laser cavity. The literature already contains $\kappa \times \omega$ Lyapunov stability diagrams [9, 10] for the representative values $B = 0.0295$, $\gamma = 0.0973$, and $\alpha = 2.6$.

A simplified proxy of the above model equations was found to have rich Lyapunov stability diagrams [7], with an extensive and intricate phase of periodic modes which, however, were not yet explored. Such proxy reads:

$$\dot{x} = \kappa + (x - \alpha y)z, \tag{4}$$

$$\dot{y} = (\alpha x - \varepsilon y)z, \tag{5}$$

$$\dot{z} = 1 - x^2 - y^2, \tag{6}$$

where $\kappa, \alpha, \varepsilon$ are real control parameters loosely related to the original parameters, and x, y, z mimic the corresponding laser variables.

For $\alpha = 3$, Li et al. [7] discovered remarkable accumulation horizons that are similar to the ones found for the state-of-the-art model of the laser [9, 10], as well as periodicity hubs [13, 14], all due to the self-organization of the oscillatory modes of the autonomous laser oscillator.

In the present work we investigate in detail the distribution of periodic oscillations for $\alpha = 3$, complementing and significantly extending the results of Li et al. [7]. Specifically, we consider how sequences of spikes unfold when two parameters are varied simultaneously. Such study led to the discovery of a large number of strongly overlapping spike-adding complexification cascades in isospike stability diagrams, which are described in what follows.

3 Isospike Stability Diagrams

Instead of Lyapunov exponents, which are computationally demanding to be generated and are only able to discriminate periodicity from lack thereof, here we use a much more fruitful representation, namely the so-called isospike stability diagrams [15–18], illustrated in Figs. 2–6. Isospike diagrams perfectly reproduce the naive dichotomic classification obtained with Lyapunov exponents. However, they are computationally less demanding to obtain and, quite significantly, contain a significant enrichment: Rather than indiscriminately bunching together all periods into a single large phase as Lyapunov diagrams do, isospike diagrams discriminate the number of spikes (local maxima) per period of each individual oscillation. As a quick glance at Figs. 2–6 unambiguously shows, isospike diagrams present detailed cartographic charts illustrating visually in a

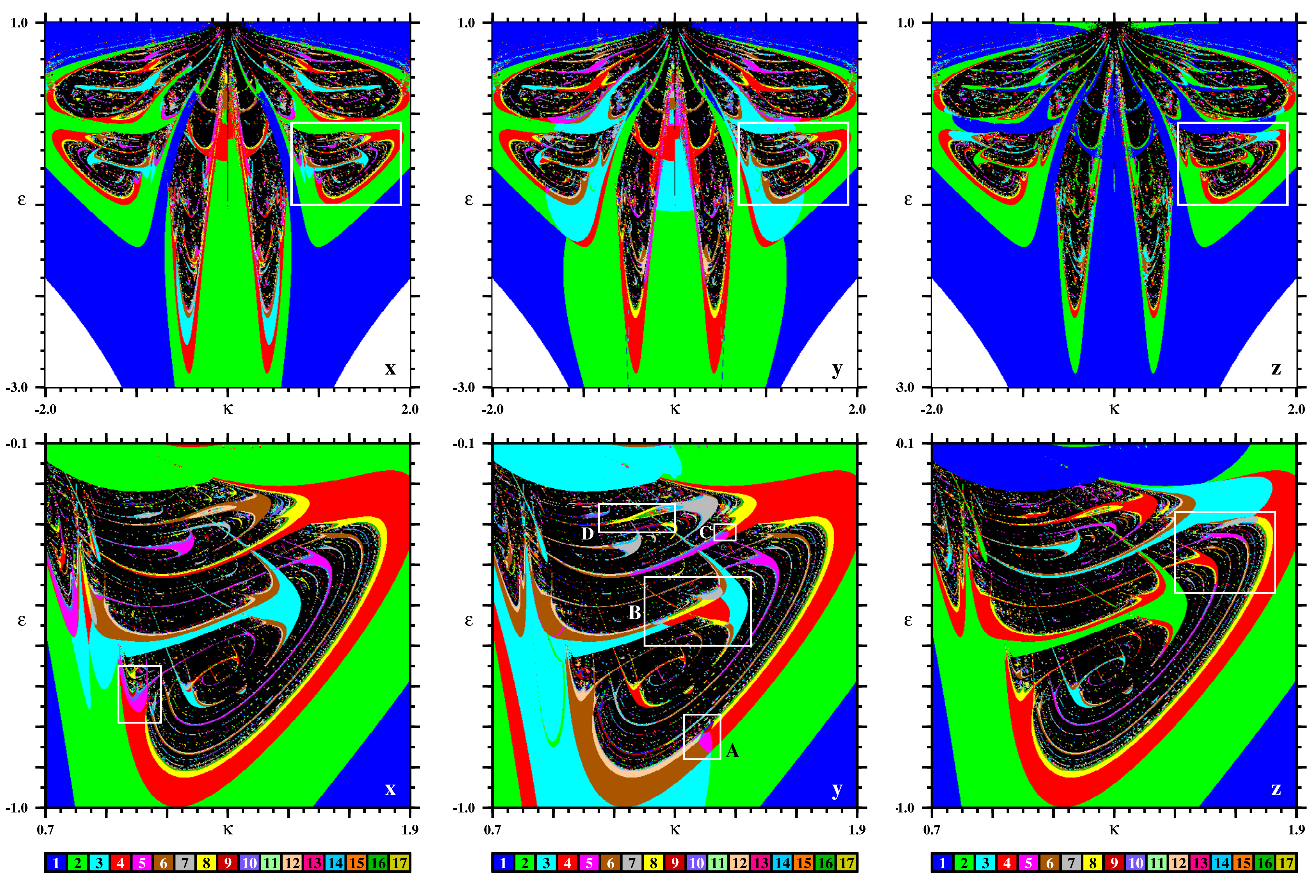

Fig. 2 Comparison of the distribution of spikes, periodic or not, as recorded in the variables x, y, z. Colors indicate the number of spikes per period of the periodic oscillations, black denotes phases of nonperiodic spiking. The white boxes on the top row are shown magnified on the bottom row. Note reflection symmetry about $\kappa = 0$, apart from the multistability. Bottom row: Boxes A,B,C,D are shown magnified in Fig. 3. The phase distributions seen in these diagrams should be compared with equivalent ones obtained for the state-of-the-art model [9, 10]

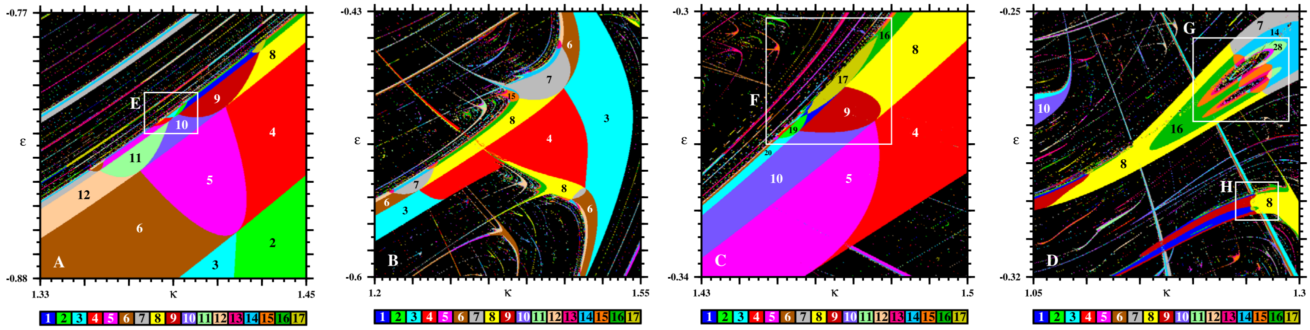

Fig. 3 Magnification of boxes A,B,C,D from Fig. 2 showing evidence of overlapping adding-doubling cascades in the y variable. Numbers refer to the number of spikes per period. After initially following the sequence illustrated in Fig. 1, the parabolic arcs begin to overlap strongly. Additional overlapping sequences exist in all panels, at smaller and smaller scales (not shown here). Boxes E,F,G are magnified in Fig. 4. Box H is magnified in Fig. 5

convenient way how complex waveforms evolve when two parameters are tuned simultaneously. For a recent survey and comparison of distinct representations of stability diagrams as well as a description about how we compute such diagrams please consult Ref. [17] and references therein.

As mentioned, a classification of stable oscillations in terms of spikes was originally introduced during a study of a three-cell population model of cancer [1], when spikes adding-doubling cascades were discovered to obey the regular nonoverlapping scheme presented in Fig. 1. Subsequently, adding-doubling cascades were also found useful to describe a large number of rather distinct systems, most recently in Refs. [2–6]. So far, the common characteristic observed in all spikes adding-doubling cascades is the presence of the nonoverlapping parabolic arcs shown in Fig. 1. As noted, complementing these earlier works, the purpose of the present paper is to report the observation of a number of rather intricate spikes adding-doubling cascades for which the parabolic arcs overlap comparatively early and extensively.

The equations of motion, Eqs. (4)-(6), were integrated using a standard fourth-order Runge–Kutta algorithm with fixed integration step $h = 0.001$, starting always from the same arbitrarily chosen initial condition $(x, y, z) = (0.1, 0.2, 0.3)$. Bitmaps were computed by "following the attractor" [17, 18] horizontally from left to right. Below, individual stability diagrams display the classification of oscillations for parameter grids containing 600×600 equally spaced points in Figs. 2, 3 and 5, and 1200×1200 points in Figs. 4 and 6.

Before proceeding, recall that in flows the period varies continuously with parameters while the number of spikes per period varies discontinuously. This means that although the addition of spikes certainly changes waveforms, in no way it affects the smooth and continuous variation of their periods. Moreover, the oscillation period is always

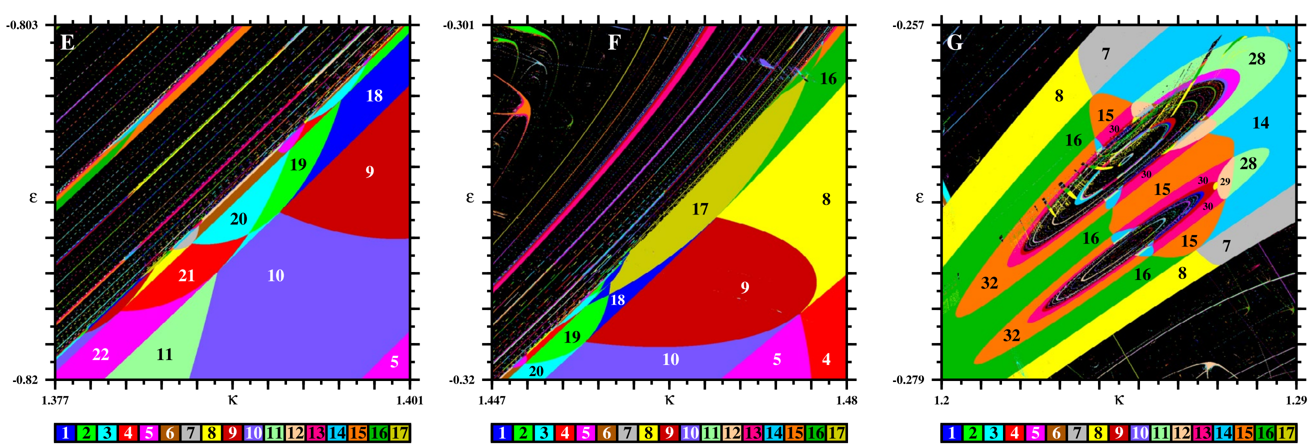

Fig. 4 Typical examples of the strong overlap of parabolic arcs observed in y spikes. Numbers refer to the number of spikes per period, with colors recycled modulo 17. Note conspicuous signs of multistability, particularly in the intricate structure in panel G, and the asymmetries of the elliptic rings embedded in the black phases of chaos. Each panel records the oscillatory behavior for a mesh containing $1200 \times 1200 = 1.44 \times 10^6$ equally spaced parameter points

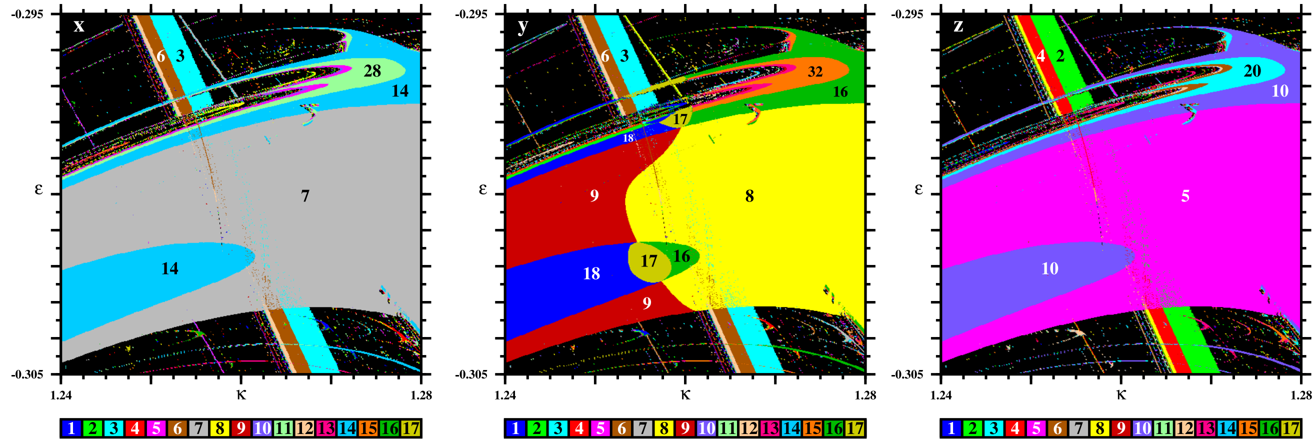

Fig. 5 Isospike phases recorded for x, y, and z. There is a "parameter bubbling" in y while spikes of x and z vary smoothly. For any set of parameters, the period measured for the three variables is always the same, independently of local variations in the number of spikes. For y, the "finger phase" combining 16, 17, and 18 spikes, seen on the lower-left corner, has the same size and shape as the corresponding phases in x and z, with 14 and 10 spikes, respectively. Note the presence of extended regions of multistability

the same, independently of the dynamical variable used to measure it and independently of the number of spikes that the individual variables may contain. Accordingly, the parabolic arcs in isospike diagrams involve spike-adding, not period-adding, the widespread use of the latter misnomer notwithstanding.

4 Results

The top row of Fig. 2 shows three stability diagrams obtained by counting spikes for the three independent variables x, y, z of the laser proxy. Such diagrams supply important information regarding the spikes distribution observed in the time-series of x, y, and z. Visually, they compare well with the two-color Lyapunov diagram computed by Li et al. [7].

In Fig. 2, notice that the inner distribution of spikes within the set U, union of all phases of periodic oscillations, may depend of the variable used to count the spikes, but not the shape or the boundary of U. Furthermore, for a fixed set of parameters, the period measured for any variable of the model is always the same, independently of the number of spikes that such variable may have. Additional details revealed by Fig. 2 are as follows.

The bottom row in Fig. 2 shows stability diagrams with white boxes focusing on some arbitrarily selected regions where the unfolding of phenomena of interest to us are easy to identify on the scales of the figure. Such boxes illustrate stability phases where the continuous evolution of the number of spikes is interrupted abruptly by the emergence of new phases with a number of spikes differing by 1 spike. For better visualization, boxes A,B,C,D are shown magnified in Fig. 3, while boxes E,F,G that Fig. 3 contains are magnified in Fig. 4.

Figures 3 and 4 show clearly that, although distorted to some extent, the adding-doubling complexification cascades follow initially the nonoverlapping scheme of Fig. 1. However, the parabolic arcs that they contain are either so close or so wide that the arcs soon start to overlap considerably in distinct ways, resulting in extended regions where additional multistability is present. Of particular interest in Fig. 3 are the boxes G and H, where complicated and symmetric self-organizations of spikes are found. In these parameter windows, triply interconnected phases induce an isomorphic repetition of the adding-doubling cascades.

So far, the emphasis was mostly on windows for a specific model variable, namely y. But, should one expect phenomena detected in y to be also detectable in other variables of the model? The answer is provided by Fig. 5 where one clearly sees this not to be the case. Two-parameter sections of multiparameter control spaces behave similarly to two-variable projections of multidimensional attractors, where each projection has its own characteristics and gives a different view of the attractor. Analogously, two-dimensional parameter sections reveal distinct features of the control parameter surface because, in general, such surface does not display a high degree of symmetry.

Figure 6 shows a most surprising self-organization of oscillation spikes that, while easy to grasp visually from the several panels, is quite difficult to summarize briefly with words. The "double-shrimp" seen in Fig. 6a involves a quite unusual and complex shrimp [17, 19–21], with "distorted" legs and a proliferation of spikes which self-organize in unusual shapes. While shrimps normally have just two regions along which chaos and doublings (of spikes in flows, and of periods in maps) occur, the stability island in Fig. 6c has a shape similar to a shrimp [17, 19–21], but, surprisingly,

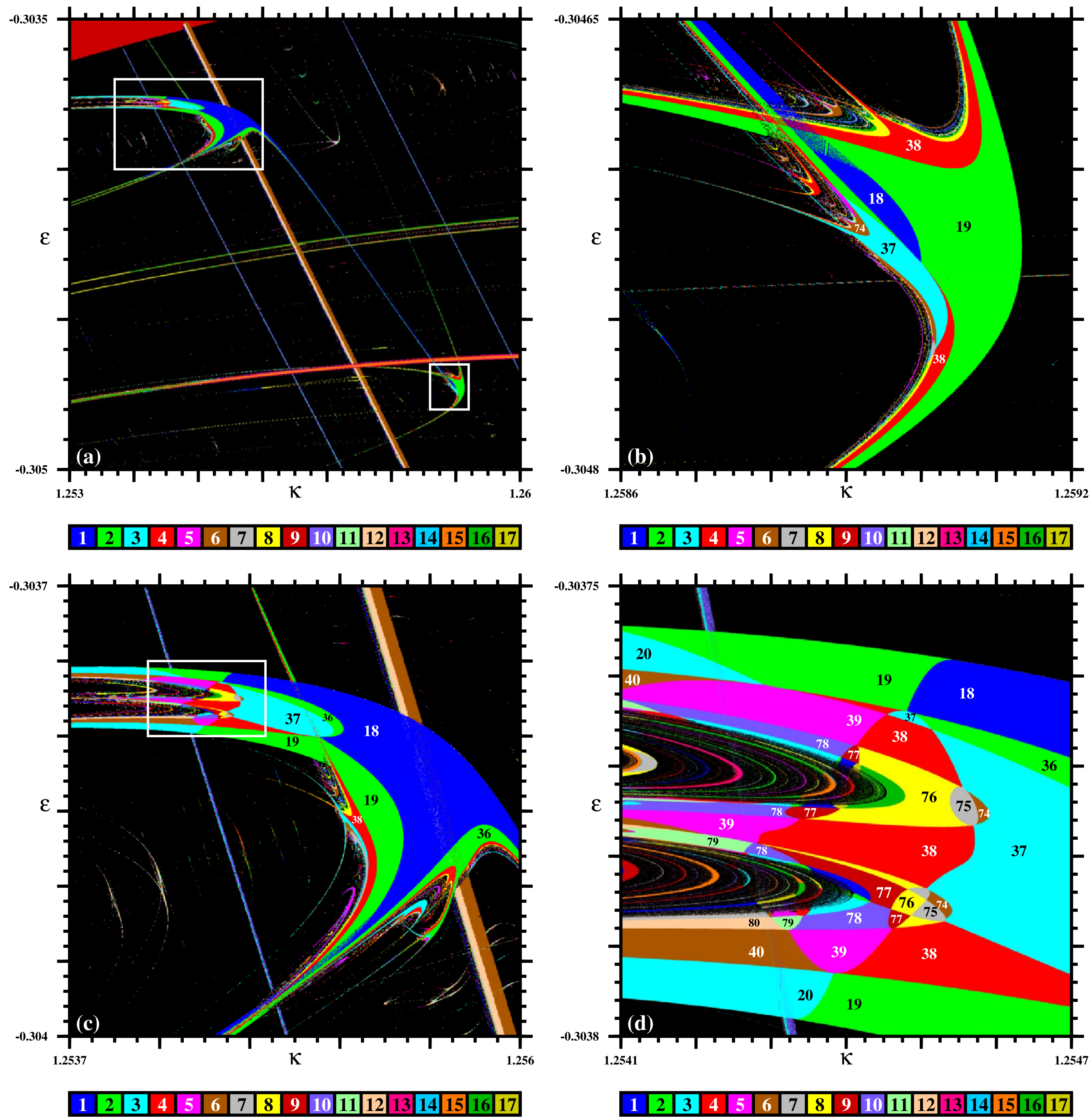

Fig. 6 Successive magnifications of complex shrimps [17, 19–21] showing parameter "bubbling" in the y variable. Numbers refer to the number of spikes per period, with colors recycled modulo 17. The larger shrimp seen in panels (a) and (c) has a subtly complex inner distribution of spikes, with three major regions where spikes cascading ending in phases of chaos occur. In (c), the white box highlights the subdivision of the upper major leg, shown magnified in (d). The spikes unfolding is considerably more complicated than the scheme in Fig. 1. Panel (d) shows a grid with $2400 \times 2400 = 5.76 \times 10^6$ parameter points. In (d), note the presence of unusually large number of spikes per period. Further adding-doubling complexification routes with an even larger number of spikes occur in the multicolored semirings embedded in the black phase of chaos

having three major chaos and doubling regions. Figure 6d illustrates the complicated and beautiful way in which spikes auto-organize. It would interesting to investigate how such mosaic of phases evolve when α is changed.

In 1984 Bier and Bountis discussed an interesting phenomenon that they called "period-bubbling" in bifurcation diagrams of maps, and for a driven Duffing equation [22]. Their bubbling phenomenon is not to be confused with the bubbling discussed subsequently in 1994 by Ashwin et al. [23]. The phenomena underlying the structure seen in the central panels in Figs. 5 and 6 are a sort of multidimensional bubbling, this time recorded exclusively in the control parameter space, similar to the re-merging that Bier and Bountis saw in the mixed space blending together variables and parameters. Depending on the specific two-parameter section of the multiparametric surface controlling the dynamics, one may see isospike cascades with a finite number of bubbles, or none at all. Manifestly, spikes cascades help to understand the intricacies underlying the control parameter surfaces of dynamical systems.

In all diagrams above, it is important to emphasize that the inner spikes distribution of the set U, representing the union of all phases of periodic oscillations, may depend on the variable used to count the spikes. However, the shape as well as the boundary of U does not depend on the variable used to count them. Furthermore, for any fixed set of parameters, the value of the period measured for each variable of the model is always the same, independently of the number of spikes that the variables may have. This fact assures that phases of nonperiodic oscillations (chaos) have the same shape and boundaries both in Lyapunov and isospike diagrams.

5 Conclusions and Outlook

This work provides a wide-ranging classifications of self-organized periodicities of various sorts as more than one control parameter is varied. So far, rhythmic, pulsating, or periodic oscillations in nonlinear oscillators have seldom been systematically followed up in any general way. Fortunately, high-performance, high-throughput computation, outperforming by wide margins everything previously available, allows the production of invaluable cartographic charts displaying detailed informations about complex systems, as illustrated by Figs. 2–6. Since the proxy model considered here essentially coincides with the state-of-the-art model of a semiconductor laser with optical injection, it is now reasonable to expect overlapping adding-doubling complexification cascades of spikes to occur in both models and to be experimentally accessible.

The main message of this paper is to draw attention to the fact that, in the same way that individual three-dimensional attractors look quite different when projected into two-dimensional sections of the space of variables, the diagrams above show two-dimensional parameter sections to display very distinct but nevertheless surprisingly regular aspects of the multidimensional control parameter surface underlying the equations of motion. The stability diagrams reported above provide an useful survey and classification of interesting facts in much need of being marshaled and brought to notice to experimentalists, and not among laser specialists only.

Clearly, it would be also interesting to explore what happens to the self-organized isospike phases described above when the parameter α is also allowed to vary, and to check how many features reported here are also present in the state-of-the-art model of a semiconductor laser with optical injection. Such questions, however, imply performing extensive computations and will be left to another opportunity. Starting Fig. 1 with p+1 and p (instead of p and p+1), produces a chiral image of the cascade. These enantiomers offer opportunities to investigate hitherto unsuspected properties of purely classical oscillators.

Acknowledgements This work was started during a visit to the Max-Planck Institute for the Physics of Complex Systems, Dresden, Germany, in the framework of the Advanced Study Group *Forecasting with Lyapunov vectors*. The author was partially supported by CNPq, Brazil, grant 304719/2015-3. All bitmaps were computed at the CESUP-UFRGS Supercomputer Center of the Federal University in Porto Alegre, Brazil.

References

1. M.R. Gallas, M.R. Gallas, J.A.C. Gallas, Distribution of chaos and periodic spikes in a three-cell population model of cancer. Eur. Phys. J. Special Topics **223**, 2131–2144 (2014)
2. X.B. Rao, X.P. Zhao, J.S. Gao, J.G. Zhang, Self-organization with fast-slow time scale dynamics in a memristor-based Shinriki's circuit. Commun. Nonlin. Sci. Num. Simul. **94**, 105569 (2021)
3. X.B. Rao, Y.D. Chu, L. Xu, Y.X. Chang, J.G. Zhang, Fractal structures in centrifugal flywheel governor system. Commun. Nonlin. Sci. Num. Simul. **50**, 330–339 (2017)
4. L. Xu, Y.D. Chu, Q. Yang, Novel dynamical scenario of the two-stage Colpitts oscillator, Chaos. Sol. Fractals **138**, 109998 (2020)
5. J.A. Vélez, J. Bragard, L.M. Pérez, A.M. Cabanas, O.J. Suarez, D. Laroze, H.L. Mancini, Periodicity characterization of the nonlinear magnetization dynamics. Chaos **30**, 093112 (2020)
6. C.S. Rodrigues, C.G.P. dos Santos, C.C. de Miranda, E. Parma, H. Varela, R. Nagao, A numerical investigation of the effect of external resistence and applied potential on the distribution of periodicity and chaos in the anodic dissolution of nickel. Phys. Chem. Chem. Phys. **22**, 21823 (2020)
7. X.F. Li, A.Y.T. Leung, Y.D. Chu, Symmetry and period-adding windows in a modified optical injection semiconductor laser model. Chin. Phys. Lett. **29**, 010201 (2012)
8. S. Wieczorek, B. Krauskopf, T.B. Simpson, D. Lenstra, The dynamical complexity of optically injected semiconductor lasers. Phys. Rep. **416**, 1–128 (2005)
9. C. Bonatto, J.A.C. Gallas, Accumulations horizons and period adding cascades in optically injected semiconductor lasers. Phys. Rev. E **75**, 055204(R) (2007)
10. C. Bonatto, J.A.C. Gallas, Accumulation boundaries: Codimension-two accumulation of accumulations in phase diagrams of semiconductor lasers, electric circuits, atmospheric, and chemical oscillators. Phil. Trans. Royal Soc. London, Series A **366**, 505-517 (2008)
11. V. Kovanis, A. Gavrielides, J.A.C. Gallas, Labyrinth bifurcations in optically injected diode lasers. Eur. Phys. J. D **58**, 181–186 (2010)

12. G.P. Agrawal, C.M. Bowden, Concept of linewidth enhancement factor in semiconductor lasers: usefulness and limitations. IEEE Photonics Technology Letters **5**, 640–642 (1993)
13. C. Bonatto, J.A.C. Gallas, Periodicity hub and nested spirals in the phase diagram of a simple resistive circuit. Phys. Rev. Lett. **101**, 054101 (2008)
14. R. Vitolo, P. Glendinning, J.A.C. Gallas, Global structure of periodicity hubs in Lyapunov phase diagrams of dissipative flows. Phys. Rev. E **84**, 016216 (2011)
15. J. Freire, J.A.C. Gallas, Stern-Brocot trees in the periodicity of mixed-mode oscillations. Phys. Chem. Chem. Phys. **13**, 12191–12198 (2011)
16. J. Freire, J.A.C. Gallas, Stern-Brocot trees in cascades of mixed-mode oscillations and canards in the extended Bonhoeffer-van der Pol and the FitzHugh-Nagumo models of excitable systems. Phys. Lett. A **375**, 1097–1103 (2011)
17. J.A.C. Gallas, Spiking systematics in some CO_2 laser models, Invited review chapter. Adv. Atom. Molec. Opt. Phys. **65**, 127–191 (2016)
18. J.A.C. Gallas, M.J.B. Hauser, L.F. Olsen, Complexity of a peroxidase-oxidase reaction model, Phys. Chem. Chem. Phys. **23**, 1943-1945 (2021).
19. J.A.C. Gallas, Structure of the parameter space of the Hénon map. Phys. Rev. Lett. **70**, 2714–2717 (1993)
20. E.N. Lorenz, Compound windows of the Hénon map. Physica D **237**, 1689–1704 (2008)
21. W. Façanha, B. Oldeman, L. Glass, Bifurcation structures in two-dimensional maps: The endoskeleton of shrimps. Phys. Lett. A **377**, 1264–1268 (2013)
22. M. Bier, T.C. Bountis, Remerging Feigenbaum trees in dynamical systems. Phys. Lett. A **104**, 239–244 (1984)
23. P. Ashwin, J. Buescu, I. Stewart, Bubbling of attractors and synchronization of chaotic oscillators. Phys. Lett. A **193**, 126–139 (1994)